Int. J. Heat Mass Transfer. Vol. 25, No. 1, pp. 127–135, 1982.
Printed in Great Britain

0017 9310/82/010127-09 $03.00/0

HEAT TRANSFER COEFFICIENTS FOR THE UPSTREAM FACE OF A PERFORATED PLATE POSITIONED NORMAL TO AN ONCOMING FLOW

E. M. SPARROW and M. CARRANCO ORTIZ
Department of Mechanical Engineering, University of Minnesota, Minneapolis, MN 55455, U.S.A.

(*Received* 21 *May* 1981 *and in revised form* 17 *July* 1981)

Abstract—Experiments were performed to determine heat transfer coefficients on an upstream-facing surface that is pierced by a regular array of holes. The holes were arranged on equilateral triangular centers, and this regular geometry gives rise to a symmetry pattern whereby each hole is surrounded by a hexagonal region, the boundaries of which are symmetry lines. Within each such hexagonal module, the heat transfer and fluid flow characteristics are identical to those of all the other modules which blanket the surface, so that measurements for a single module yield information for the entire surface. This feature has been employed in the design and execution of the present experiments. Two parameters were varied during the course of the experiments the hole pitch-to-diameter ratio P/D and the per-hole Reynolds number Re. The results were tightly correlated by the relation $Nu_{L^*} = 0.881 Re^{0.476} Pr^{1/3}$. The characteristic dimension in the Nusselt number is the ratio of the module surface area to the pitch, while the Reynolds number is that for flow through a pipe having a diameter equal to that of the holes in the plate. Flow visualization studies confirmed the existence of the array of hexagonal modules.

NOMENCLATURE

- A, surface area of module;
- D, hole diameter;
- $\mathscr{D}$, naphthalene–air diffusion coefficient;
- h, heat transfer coefficient;
- K, mass transfer coefficient, equation (3);
- k, thermal conductivity;
- L^*, characteristic length, A/P;
- $\dot{M}$, rate of mass transfer, $\Delta M/\tau$;
- ΔM, change in mass due to sublimation;
- Nu_{L^*}, Nusselt number based on L^*, hL^*/k;
- Nu_p, Nusselt number based on P, hP/k;
- P, pitch, Fig. 1;
- Pr, Prandtl number;
- p_{nw}, naphthalene vapor pressure at surface;
- Re, per-hole Reynolds number, equation (6);
- Sc, Schmidt number, $\nu/\mathscr{D}$;
- Sh_{L^*}, Sherwood number based on L^*, $KL^*/\mathscr{D}$;
- Sh_p, Sherwood number based on P, $KP/\mathscr{D}$;
- $\dot{w}$, rate of mass flow through entire array.

Greek symbols

- μ, viscosity;
- ν, kinematic viscosity;
- ρ_{nw}, density of naphthalene vapor at the surface;
- $\rho_{n\infty}$, density of naphthalene vapor in approach flow;
- τ, duration of data run.

INTRODUCTION

THERE is a diversity of physical situations where fluid from an upstream space passes into a regular array of holes which pierce a surface that faces the upstream space. Such a configuration occurs, for example, at the upstream tubesheet of a shell and tube heat exchanger. Another example is encountered in the making of fiberglass threads, where molten glass is withdrawn from a containment vessel through a regular array of holes in the floor of the vessel. Numerous other applications are encountered in connection with the widespread use of perforated plates in process industries and as devices to smooth non-uniformly distributed flows.

When the temperature of the upstream-facing surface is different from that of the oncoming fluid, heat will be transferred as the fluid passes over the surface en route to the holes. It is this transfer of heat that is the focus of the present study. The investigation has two parts. In the first part, heat transfer coefficients for the upstream-facing surface are determined experimentally, while the second is a flow visualization aimed at examining the pattern of fluid flow adjacent to the surface. Despite the numerous practical applications to which the results are relevant, it is remarkable that a survey failed to reveal any heat

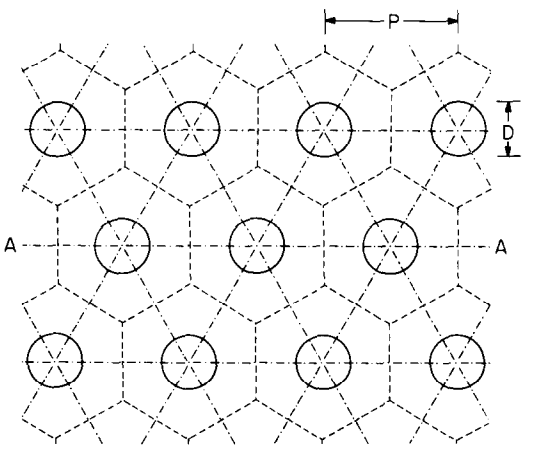

FIG. 1. Equilateral triangular array of holes showing the pattern of hexagonal symmetry.

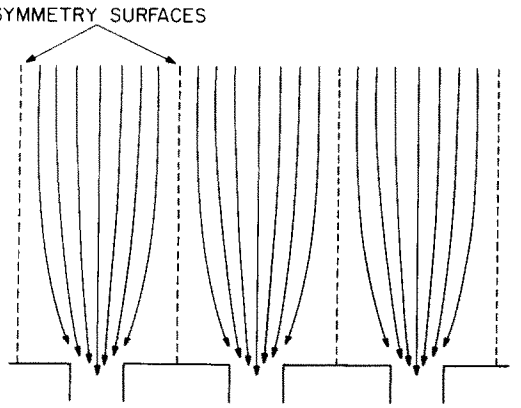

FIG. 2. Schematic view of the pattern of fluid flow passing from the upstream space into the holes along section A–A (section A–A is defined in Fig. 1).

transfer coefficient information in the published literature for an upstream facing surface pierced by a regular array of holes.

In this investigation, consideration will be given to upstream-facing surfaces pierced by holes that are deployed in an equilateral triangular pattern. Such an arrangement is pictured schematically in Fig. 1, which is intended to portray an array containing a sufficiently large number of holes so that end effects are negligible at holes that are situated in the central portion of the array. The equilateral triangular pattern possesses symmetry properties that are illustrated in the figure. As shown there, each of the holes is surrounded by a hexagonal region, the boundaries of which (shown as dashed lines) are symmetry lines with regard to the fluid flow. These hexagons are constructed by drawing connecting lines between the centers of the holes, as in the figure. In reality, the symmetry lines which comprise the hexagons are actually symmetry surfaces which extend upstream from the plate into the space from which fluid is drawn into the holes. This is illustrated in Fig. 2, which shows a schematic view of the pattern of fluid flow passing from the upstream space into the holes along section A–A (section A–A is defined in Fig. 1).

In view of the foregoing considerations, the entire flow field can be regarded as being subdivided into an ensemble of hexagonal cells (or modules), with the flow pattern in each cell being the precise duplicate of that in every other cell. Furthermore, fluid does not cross the symmetry surfaces, such that the flow field in each cell is independent of that in the others.

Next, with regard to the heat transfer, it is apparent that if the surface of the upstream-facing plate is isothermal (as is the case in the present investigation), then the aforementioned velocity symmetry lines are also symmetry lines for the temperature field. As a consequence, there is no heat transfer by conduction across the symmetry lines which lie in the surface of the plate nor is there convective or conductive heat transfer across the symmetry surfaces that extend upstream from the plate into the space from which the fluid is drawn.

These considerations indicate that if the heat transfer characteristics were to be determined for the hexagonal region that surrounds one of the holes of the array, then the average heat transfer coefficient for that hexagon is precisely equal to the average heat transfer coefficient for the entire upstream-facing surface. Accordingly, in the experiments as actually performed, heat transfer coefficients were determined at only one of the typical hexagons, hereafter referred to as the active module.

To take advantage of the symmetry considerations that have been discussed in the foregoing, it was natural to use the naphthalene sublimation technique in lieu of direct heat transfer measurements, and then to convert the mass transfer results to heat transfer results via the well established analogy between the two processes. The validity of the analogy has been firmly established both on a first-principles basis [1] and by numerous comparisons with experimental correlations and analytical predictions for heat transfer. The overwhelming advantage of the naphthalene technique in the present instance is that it enables the symmetry lines which envelop the active module to truly correspond to boundaries of zero mass transfer (i.e. by the analogy, to boundaries of zero heat transfer). If, on the other hand, the experiments were to be performed for a single active module by means of direct heat transfer measurements, it would be unlikely that the symmetry lines would be strictly adiabatic because thermal insulators of the requisite quality do not exist. Other advantages of the naphthalene technique include the high accuracy which it affords and the relative simplicity of the apparatus which is needed for its utilization.

The flow visualization studies were performed using the oil–lampblack technique. The main objective of the visualization was to verify the existence of a hexagonal symmetry envelope around the active module.

Two parameters were varied during the course of the investigation. One of these is the pitch-to-diameter ratio P/D, where P and D are illustrated in Fig. 1. The other parameter is the Reynolds number, which was varied over a range encompassing an order of magnitude. Auxiliary experiments were also carried out to assess the effect of the number of holes in the experimental array on the heat transfer coefficients measured at the active module. Air was the working fluid for all the experiments.

THE EXPERIMENTS

Apparatus overview and design.

The description of the experimental apparatus is facilitated by reference to Fig. 3. As shown schematically in the upper diagram of the figure, a disk containing the array of holes is positioned in the upper wall of a large plenum chamber. Air is drawn from the laboratory room into the plenum chamber through the

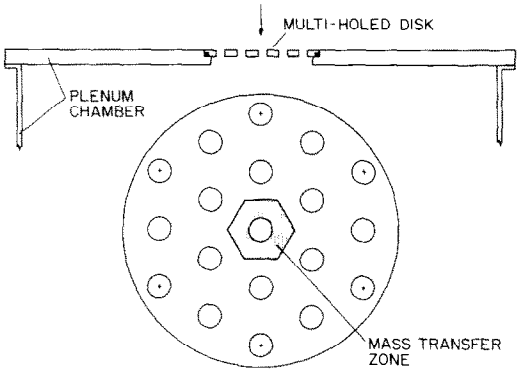

FIG. 3. Upper diagram: multi-holed disk positioned in the upper wall of a large plenum chamber; lower diagram: front-face view of the multi-holed disk with $P/D = 2.5$.

multi-hole array by a blower(s) positioned downstream of the plenum. Thus, the surface of the disk which faces the laboratory room is the upstream-facing surface on which the heat transfer coefficients are being sought.

The lower diagram of Fig. 3 is a front-face view of one of the multi-holed disks that were employed during the experiments. As noted earlier, the holes are arranged in an equilateral-triangular pattern. The main feature of this diagram is the hexagonal region which surrounds the center hole of the array. As can be seen in the diagram, the space between the hexagon and the hole is filled with solid naphthalene, the sublimation of which yields the mass transfer data and, by analogy, the desired heat transfer data.

There were a number of factors which had to be taken into account in selecting the three geometrical parameters of the array—the hole diameter D, the pitch P, and the number of holes N. The major challenge was to obtain values of P/D which lie at the low end of the practical range (~ 1.5) [2] and to obtain Reynolds numbers Re at the high end of the range ($\sim$ 40,000) [3]. Larger P/D and smaller Re posed no difficulties.

The design considerations will now be described. For the experimental apparatus, the maximum per-hole Reynolds number Re_{max} may be written in terms of the maximum mass flow rate $\dot{w}_{max}$ that can be provided by the air-handling system, the number of holes N, and the hole diameter D:

$$Re_{max} = 4(\dot{w}_{max}/N)/\mu\pi D. \quad (1)$$

Based on equation (1), a strategy for obtaining as large a Reynolds number as possible would be to use relatively few holes (i.e. small N), each of small diameter D.

There are two factors that, however, conflict with the choice of small N and small D. One of these is the requirement that the experimental array consist of a sufficiently large number of holes so that the finiteness of the array has only a minimal effect on the mass transfer coefficients measured at the active module. The other consideration has to do with the desired accuracy of the naphthalene mass transfer measurements. The amount of mass ΔM sublimed during a data run is

$$\Delta M = \rho_s A \delta \quad (2)$$

where ρ_s is the density of the solid naphthalene, A is the surface area of the naphthalene exposed to the airflow, and δ is the mean recession due to sublimation during the data run. In order to maintain the basic geometric configuration, it is reasonable to limit δ to 0.00254 cm (0.001 in.). Furthermore, the resolving power of the available analytical balance is 0.1 mg, so that uncertainties of 0.2–0.4 mg are possible for a data run owing to the multiple weighings that are made. Thus, for 2% accuracy, ΔM should be about 15 mg. This requirement sets a lower bound on the area A of the naphthalene surface exposed to the airflow. Therefore, if D is small and if P/D is also small, then the area A is smaller than the permitted lower bound.

On the basis of the available air supply (130 scfm maximum volume flow) and the perceived need (based on the visual examination of various array layouts) to use at least 19 holes to model an infinite array, calculations showed that per-hole Reynolds numbers as large as 20,000 could be obtained for P/D ratios of 2.0 and 2.5, while fulfilling the accuracy requirement for the mass transfer measurement. These pitch-to-diameter ratios were employed during the course of this research. The resulting hole sizes corresponding to $P/D = 2.0$ and 2.5 were 1.27 cm and 1.17 cm (0.500 and 0.460 in.), respectively.

The layout for the $P/D = 2.5$ case is illustrated in the lower diagram of Fig. 3. In an auxiliary set of data runs, performed to examine the effect of the number of holes, certain of the holes were closed, and these are designated by the cross symbols in Fig. 3.

Apparatus details

The upper wall of the plenum chamber, which served as the host surface for the multi-holed disk, was a 61×61 cm (2×2 ft) square aluminium plate, 1.27 cm ($\frac{1}{2}$ in.) thick. A 13.97 cm (5.50 in.) diameter opening, fitted with a lap, was machined centrally into the wall to accommodate the disk. The plenum was 1.2 m (4 ft) in height. At its base surface, it was equipped with a pipe stub which facilitated connection to the air-handling system.

Each of the two disks was made to fit precisely into the opening in the upper wall of the plenum, with positive sealing being provided by an O-ring positioned in a groove along the outer rim of the lower surface of the disk. The compression of the O-ring was accomplished by the tightening of screws, via access from below through a port in the plenum sidewall. Both disks were of aluminium, 0.495 cm (0.195 in.) thick. When in place, the exposed surface of the disk was precisely coplanar with that of the plenum wall.

To accommodate the mass transfer zone which surrounds the center hole, a cavity, 0.292 cm (0.115 in.) deep, was milled into the disk with the aid

of a rotary table placed on the bed of a vertical milling machine. A special machining operation was used to ensure sharp (unrounded) corners at each of the vertices of the hexagon.

With regard to the containment of the naphthalene in the hexagonal cavity, the inner boundary of the cavity was a thin-wall sleeve whose bore served as the aperture through which fluid passed into the center hole of the array. Such a sleeve was used to avoid the configuration in which the naphthalene itself bounds the aperture. Had the sleeve not been used, the aperture opening would have enlarged during the course of the data run and become bell mouthed. The sleeve was made as thin as possible consistent with strength and life considerations, and served to maintain a square-edged aperture of fixed diameter. The thickness of the sleeve exposed to the airflow was 0.025 cm (0.010 in.) for both plates.

With respect to the flow circuit, the air drawn from the laboratory room through the plenum exited from the plenum base, from which point it passed into the rotameters, valves, and blowers. The blowers were situated in a service corridor adjacent to the laboratory, and their exhaust was vented outside the building. The outside exhaust guaranteed that the air drawn toward the test section was free of naphthalene vapor. Furthermore, operation of the apparatus in the suction mode ensured that the temperature of the air passing over the naphthalene surface was always the same as the air in the room, which was controlled and maintained at about 22°C (71°F). Two blowers, ranged in parallel, served to induce the airflow, with a separate calibrated rotameter used in conjunction with each blower.

The air temperature was monitored by an ASTM-certified thermometer which could be read accurately to within 0.025°C (0.05°F). The amount of naphthalene sublimed during each run was determined by weighing the multi-holed disk before and after the run using a Sartorius precision analytical balance accurate to 0.1 mg for specimens up to 200 g.

Naphthalene test surfaces

The naphthalene test surface was fabricated by a casting process using a two-part mold. One part of the mold was the disk itself, and the other part was a thick, highly polished stainless steel plate. To initiate the casting procedure, the naphthalene remaining in the disk from a prior data run was removed by melting and subsequent evaporation. The disk was then placed on the thick stainless steel plate with the open face of the hexagonal cavity downward. Then, previously unused, reagent-grade molten napththalene was poured into the cavity through an access aperture in the rear face of the disk. Three smaller apertures enabled escape of the air which was displaced by molten naphthalene. After the hexagonal cavity had been filled and the naphthalene had solidified and cooled, the disk was separated from the stainless steel plate.

Upon the completion of the casting procedure, the naphthalene surface was carefully protected against sublimation with a hexagonally shaped impermeable plastic cover. The pouring apertures were also covered with impermeable tape in order to prevent extraneous sublimation during the data run. The test plate sealed thus was placed in the laboratory to attain thermal equilibrium.

Experimental procedure

To prepare for a data run, the flow rate was initiated and the room lighting turned on at least one hour before the intended start of the run. During this period, the plate was positioned in its recess in the upper wall of the plenum, the naphthalene test section still being protected against sublimation by the plastic cover, and air was drawn through all the holes except the centermost, which was closed. This period enabled steady-state operation of the blower(s) to be achieved and thermal equilibrium between the airflow and the test surface to be attained.

Immediately before the data run, the disk was weighed (subsequent to the removal of the protective plastic cover). Then, after the weighing, a specially fabricated Teflon cover capable of rapid installation was placed over the naphthalene surface. This cover was kept in place while the disk was implanted and secured in its recess in the upper wall of the plenum.

During the course of the run, the air temperature, the flow rate(s), and the related pressure(s) were closely monitored and recorded. The durations of the data runs were selected so that the mean depression of the naphthalene surface would not exceed 0.00254 cm (0.001 in.). At the typical temperature level of the laboratory (22°C, 71°F), the run durations ranged from 30 to 80 minutes, and the change of mass during a run was in the range from 13 to 19 mg.

The termination of each data run was defined by the simultaneous replacement of the Teflon cover on the naphthalene test surface and the deactivation of the timer and the blower(s). The disk was weighed immediately after the run.

To determine the magnitude of any extraneous sublimation that may have occurred during the set-up and disassembly of the experiment, a mock data run was executed subsequent to the after-weighing. Specifically, all steps in the set-up and disassembly periods were repeated, except that the naphthalene was not exposed to the airflow. The change of mass during the mock experiment was taken to be equal to the extraneous mass transfer during the actual experiment. Typically, the correction due to the extraneous transfer was 0.2 mg.

Flow visualization

The oil–lampblack technique was employed to enable visualization of the flow field adjacent to the test surface. Lampblack is a very fine black powder which mixes readily with oil, and the mixture, when brushed on a surface, produces a smooth, glossy black coating. The general procedure for using this tech-

nique is to brush the oil–lampblack mixture on a surface and then to expose the surface to the airflow whose characteristics are to be studied. Ideally, under the action of the shear stresses exerted by the flow, the mixture will move along the surface, following the paths of the fluid particles that pass adjacent to the surface. These path lines will appear as streaks on the surface. In regions of low velocity, the shear stresses are small and the mixture will remain stationary, so that such regions show themselves as black streak-free zones on the surface.

To facilitate the visualization, a number of oils of various viscosities were assembled, and numerous trial mixtures were employed in preliminary visualization runs. For all the visualization runs, both preliminary and final, the face of the disk was coated with white, plasticized contact paper in order to provide the highest possible contrast for the black streak lines induced on the surface by the flow. In order to obtain the clearest possible patterns, the final visualization runs were made at the highest Reynolds number studied, namely a per-hole Reynolds number of about 20,000. From the preliminary runs, it was found that the flow pattern observed at this Reynolds number persisted at all the Reynolds numbers for which patterns could be obtained. Photographs were taken of the flow patterns thus visualized, and an illustrative one will be presented later.

DATA REDUCTION

The procedure used to deduce mass transfer coefficients and their dimensionless counterpart, the Sherwood number, from the measurements of mass, run time, and temperature will now be described, as will the determination of the Reynolds number. To this end, let ΔM denote the change of mass during a data run (corrected as described earlier) and let τ denote the duration of the run, so that $\Delta M/\tau = \dot{M}$ is the rate of mass transfer. Then, the average mass transfer coefficient K for the hexagonal module can be written as

$$K = \frac{\dot{M}/A}{\rho_{nw} - \rho_{n\infty}}. \tag{3}$$

In this equation, A is the area of the surface which participates in the mass transfer process, while ρ_{nw} and $\rho_{n\infty}$ are the densities of naphthalene vapor at the surface and in the approach flow.

The quantity $\rho_{n\infty}$ is zero in the present experiments, while ρ_{nw} is determined by a two-step computation. The first step yields the vapor pressure p_{nw} at the surface corresponding to an input value of the surface temperature [4], and with p_{nw} and the surface temperature, ρ_{nw} is calculated from the perfect gas law. For these calculations, it was assumed that the surface temperature is equal to the measured air temperature, and the validity of this assumption will now be established.

One cause of possible deviations between the surface and ambient temperatures stems from the latent heat requirements of the sublimation process. If it is assumed that the latent heat is supplied solely by convective heat transfer from the airflow, then an energy balance can be written as

$$hA\Delta T = \dot{M}\lambda \tag{4}$$

where the left-hand side is the rate of convective heat transfer and the right-hand side is the rate of latent heat utilization, with λ denoting the latent heat of sublimation and h denoting the convective heat transfer coefficient; ΔT is the difference between the ambient and surface temperatures. The h values needed to evaluate equation (4) were determined by applying the heat/mass transfer analogy to the mass transfer coefficients measured during the present experiments. Evaluation of equation (4) yields $\Delta T = 0.075$°C (0.14°F) for the operating conditions of the experiments. Because of other energy inputs omitted from equation (4), the aforementioned value of ΔT is an upper bound. Measurements in a related experiment in which thermocouples could be conveniently installed yielded $\Delta T = 0.045$°C (0.08°F).

Another possible source of error is that the measured air temperature corresponds to the stagnation temperature, while the surface temperature may be closer to the recovery temperature. The difference between these temperatures depends on the air velocity passing over the surface. At the highest velocity of the experiments, the stagnation temperature was calculated to be 0.075°C (0.14°F) larger than the recovery temperature. In the middle of the velocity range, the corresponding difference is 0.019°C (0.035°F).

The aforementioned differences between the measured air temperature and the surface temperature of the naphthalene give rise to uncertainties of 1% or less in ρ_{nw}.

Once the mass transfer coefficient has been determined, the Sherwood number may be evaluated from

$$Sh = KL/\mathscr{D} \tag{5}$$

where $\mathscr{D}$ is the naphthalene–air diffusion coefficient, and L is a characteristic dimension which will be specified during the presentation of results. The diffusion coefficient was evaluated via the Schmidt number $Sc = \nu/\mathscr{D}$, with $Sc = 2.5$ [4] and ν equal to the kinematic viscosity of air.

For the Reynolds number, it is believed that the pipe-flow Reynolds number, based on the hole diameter and the per-hole mass flow, will have greater meaning both to practitioners and researchers than alternative definitions. For instance, for shell and tube heat exchangers, the Reynolds number of the tubes which are fed by fluid passing through the holes in the tubesheet would be known. To evaluate such a Reynolds number definition, the measured mass flow for the 19-hole array was prorated uniformly among the holes, yielding $\dot{w}/19$ for each hole, and the hole diameter D was employed as the characteristic

dimension, so that

$$Re = 4(\dot{w}/19)/\mu\pi D. \quad (6)$$

The results will be correlated in the form $Sh = f(Re)$ and, subsequently, by applying the heat/mass transfer analogy, a correlation in the form $Nu = f(Re, Pr)$ will be presented, where Nu is the average Nusselt number.

RESULTS AND DISCUSSION

Mass (heat) transfer results

The results for the average mass transfer coefficient for the hexagonal module will now be presented. In the initial presentation of these results, the Sherwood number will be based on the pitch P as the characteristic dimension, so that $Sh_p = KP/\mathscr{D}$. The use of the pitch has the virtue of simplicity (as compared to other candidate characteristic lengths that are combinations of dimensions) and, in addition, the magnitude of P can serve as an index of the size of the hexagonal module.

In Fig. 4, Sh_p is plotted as a function of the Reynolds number, which covers the range of 2000–20,000. The results for the pitch-to-diameter ratios P/D of 2.0 and 2.5 are respectively represented by blackened and open circles. All of the data represented by circular symbols correspond to an array consisting of 19 holes. Data from auxiliary runs made with a 13-hole array are designated by square symbols.

As seen in the figure, the Sherwood number increases in a regular manner with the Reynolds number for both of the P/D ratios investigated. Within the scatter of the data, the Sh_p, Re relation for each P/D can be very well represented by a straight line, and least-squares fits yielded $Nu_p = 1.90Re^{0.469}$ and $Nu_p = 1.52Re^{0.483}$, respectively for $P/D = 2.0$ and 2.5. The Reynolds number exponents for the two cases differ only slightly, and the difference is probably not significant within the scatter of the data. Therefore, a common exponent equal to the mean value of the aforementioned individual exponents was employed (= 0.476).

With this, least-squares fits yielded

$$Sh_p = Nu_p = 1.78\,Re^{0.476}, \quad P/D = 2.0 \quad (7)$$

$$Sh_p = Nu_p = 1.62\,Re^{0.476}, \quad P/D = 2.5 \quad (8)$$

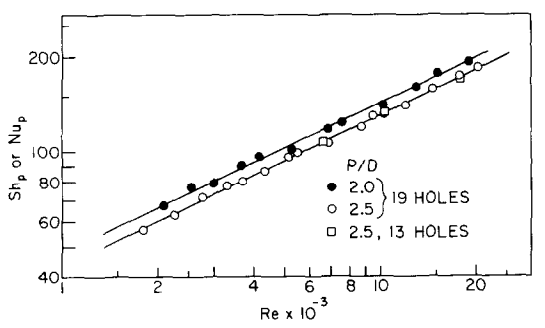

FIG. 4. Mass (heat) transfer results for $P/D = 2.0$ and 2.5; the characteristic dimension in the Sherwood number is the pitch P.

where the analogy between heat and mass transfer has been invoked. The straight lines appearing in Fig. 4 are representations of equations (7) and (8). As written, equations (7) and (8) apply specifically for $Sc = 2.5$ and $Pr = 2.5$; generalization to heat transfer situations characterized by other Prandtl numbers will be made shortly.

It is interesting to note that the Reynolds number exponent, 0.476, which appears in equations (7) and (8) is not very different from the value of 0.5 which characterizes simple laminar stagnation flows. The present flow field has some features in common with a stagnation flow and, for example, the dashed lines appearing in Fig. 2 can be regarded as stagnation streamlines. However, the turning of the flow as it enters the holes is a unique feature not found in stagnation flows.

Another interesting aspect of equations (7) and (8) is the modest difference—about 9.4%—between the numerical constants in the two equations. Thus, it appears that the use of the pitch P as the characteristic dimension in the Sherwood (or Nusselt) number is quite effective in muting the dependence of the results on the P/D ratio. In the interests of a concise and simple presentation, a representation accurate to better than $\pm 5\%$ over the range $2.0 \leq P/D \leq 2.5$ can be written as

$$Sh_p = Nu_p = 1.70Re^{0.476}. \quad (9)$$

Notwithstanding the foregoing, it was deemed desirable to examine the use of other characteristic dimensions to see if a correlation could be achieved which is independent of P/D. Such a correlation would facilitate interpolation and extrapolation of the results to P/D values other than those employed here.

The first alternative characteristic dimension to be examined is one which has the form of a hydraulic diameter, but without its physical significance. A pseudo hydraulic diameter may be defined as the surface area A of the mass transfer module divided by the perimeter which bounds the area A (the perimeter includes both the hexagon and hole perimeters). When such a characteristic dimension is used in the Sherwood number, the constants in the individual correlations corresponding to $P/D = 2.0$ and 2.5 differ by 6.9%. Compared with equations (7) and (8), this represents a slight coalescing of the correlating equations, but at the price of a much more complex characteristic dimension. It is interesting to note that if the pseudo-hydraulic diameter is used in both the Sherwood and Reynolds numbers, the spread between the correlating equations becomes appreciably larger.

From further study, it was found possible to bring the data for both P/D ratios together onto a single line by defining a characteristic length L^* as

$$L^* = A/P \quad (10)$$

and employing it in the Sherwood number, while maintaining the diameter D as the characteristic length

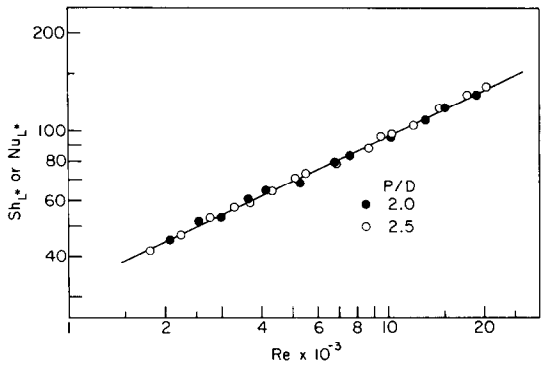

FIG. 5. Mass (heat) transfer results for $P/D = 2.0$ and 2.5; the characteristic dimension in the Sherwood number is $L^* = A/P$.

in the Reynolds number. The single correlation which results is

$$Sh_{L^*} = Nu_{L^*} = 1.196Re^{0.476}. \quad (11)$$

This equation has been plotted in Fig. 5 along with the experimental data. It is seen that equation (11) provides an excellent representation of the data, and its use is recommended both for interpolation within the range $2.0 \leq P/D \leq 2.5$ and for moderate extrapolations outside that range.

Attention will now be turned to the generalization of the correlating equations, either (9) or (11), to apply to other Prandtl numbers. For external flows, it is common to express the Prandtl number dependence in the form $Nu \sim Pr^{1/3}$ at a fixed Reynolds number, although Zukauskas [5] suggests that an exponent of 0.36–0.37 is more suitable. If the 1/3 power is used, then equations (9) and (11) become

$$Nu_p = 1.25Re^{0.476}\,Pr^{1/3}, \quad (12)$$

$$Nu_{L^*} = 0.881Re^{0.476}\,Pr^{1/3} \quad (13)$$

where equation (13) is preferred for extrapolation and interpolation with respect to P/D.

As the final item in the discussion of the mass (heat) transfer results, consideration will be given to the data for the thirteen-hole array that appear in Fig. 4. The 13-hole array was obtained by closing the six outermost holes (those designated by cross symbols in Fig. 3) of the original $P/D = 2.5$ array with adhesive tape. The 13-hole experiments were undertaken to examine the response of the Sherwood–Reynolds relation to the number of holes since, in the data reduction procedure, it was assumed that the total mass flow is prorated equally among all the holes in the disk. If the experimental data for a lesser number of holes were to not deviate from the data obtained for the 19-hole array, then any departures from uniform prorating of the flow could be regarded as negligible.

As seen in Fig. 4, there is no discernible difference between the results for the 13- and 19-hole arrays. This finding lends strong support to the notion that the results reported here are uninfluenced by the finite size of the experimental array.

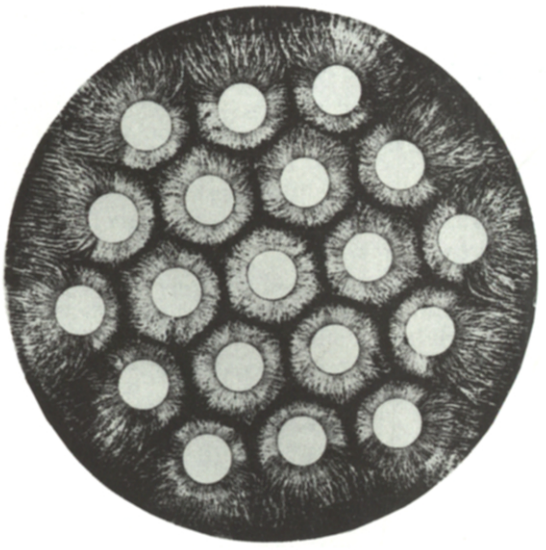

FIG. 6. Pattern of fluid flow adjacent to the surface of a multi-holed disk with $P/D = 2.0$.

Flow visualization

The flow visualization studies were performed using the same multi-holed disks as were employed in the mass transfer experiments, but with the surface covered with white, plasticized contact paper. Holes were cut in the contact paper to coincide with those in the disk. Visualization patterns were obtained for both the $P/D = 2.0$ and 2.5 disks, both with 19 holes, and for the $P/D = 2.5$ disk with 13 holes. All of the visualization patterns yielded the same basic message and, therefore, only a typical pattern, that for $P/D = 2.0$, will be presented in Fig. 6.

Inspection of Fig. 6 shows that, indeed, there are hexagonal regions around the holes. Since the boundaries of the hexagons are formed by lines of flow stagnation, these boundaries are shown as black lines by the oil–lampblack technique. The hexagon surrounding the center hole is perfectly symmetric. Furthermore, the central hexagon is surrounded by six complete hexagons which, with respect to the center hole, simulates the situation that would prevail in an infinite array. Thus, the mass (heat) transfer results for the hexagon surrounding the center hole can be regarded as representative of those for a typical hole in an effectively infinite array.

Owing to the finiteness of the array, some asymmetry in the shapes of the hexagons is in evidence in the direction from the center of the array toward the outer holes. The hexagons for the outermost holes are, necessarily, incomplete.

The streak lines show the details of the flow pattern adjacent to the surface. From these, it can be seen that near the surface, the flow toward each of the holes is more or less radial.

CONCLUDING REMARKS

The heat (mass) transfer coefficients reported here

should be of direct applicability to the thermal design of perforated plate systems, with the recommended Nusselt–Reynolds–Prandtl relation being $Nu_L^* = 0.881 Re^{0.476} Pr^{1/3}$. This relation is based on experiments which extended over an order of magnitude in Reynolds number ($2000 \leq Re \leq 20{,}000$). The close adherence of the heat (mass) transfer data to a power law dependence upon the Reynolds number throughout this entire range suggests that the aforementioned correlation can be employed at higher Reynolds numbers with an expectation of satisfactory accuracy.

Although the range of pitch-to-diameter ratios employed in the experiments was modest ($2.0 \leq P/D \leq 2.5$), the fact that the correlating equation is independent of P/D provides encouragement for its application to a wider range of P/D values. The selection of the $Pr^{1/3}$ power law for generalizing the basic data, which correspond to $Pr = 2.5$, was based on the wide utilization of this power law for external flows. In the recent literature, there is some preference for an exponent of 0.36 or 0.37 instead of 1/3. Had $Pr^{0.37}$ been used in the correlating equation, the constant 0.881 would be replaced by 0.852.

Acknowledgement—This research was performed under the auspices of the National Science Foundation. Scholarship support was accorded to M. Carranco Ortiz by CONACYT, Mexico.

REFERENCES

1. E. R. G. Eckert, Analogies to heat transfer processes, in *Measurements in Heat Transfer* (Edited by E. R. G. Eckert and R. J. Goldstein). Hemisphere, Washington, D.C. (1976).
2. *Standards of Tubular Exchanger Manufacturers Association* (6th edn.) Tubular Exchanger Manufacturers Association, New York (1978).
3. D. Q. Kern, *Process Heat Transfer*. McGraw-Hill, New York (1950).
4. H. H. Sogin, Sublimation from disks to airstreams flowing normal to their surfaces, *Trans. Am. Soc. mech. Engrs* **80**, 61–71 (1958).
5. A. A. Zukauskas, Heat transfer from tubes in crossflow, *Adv. Heat Transfer* **8**, 93–160 (1972).

COEFFICIENT DE TRANSFERT THERMIQUE POUR LA FACE AMONT D'UNE PLAQUE PERFOREE NORMALE A UN ECOULEMENT INCIDENT

Résumé—Des expériences permettent de déterminer les coefficients de transfert thermique sur une surface faisant face à un écoulement et percée d'un réseau régulier de trous. Les trous sont disposés selon une maille en triangle équilatère et cette géométrie conduit à une symétrie telle que chaque trou est entouré par une région hexagonale dont les frontières sont des lignes de symétrie. Le transfert thermique et les caractéristiques de l'écoulement sont identiques pour toutes les mailles, de telle sorte que les mesures pour une seule donnent information pour la surface entière. Deux paramètres sont variables durant les expériences, le rapport pas sur diamètre des trous P/D et le nombre de Reynolds Re relatif au trou. Les résultats sont étroitement représentés par la relation $Nu_L = 0{,}881\ Re^{0.476}\ Pr^{1/3}$. La dimension caractéristique dans le nombre de Nusselt est le rapport de la surface de la maille au pas, tandis que le nombre de Reynolds est celui de l'écoulement à travers un tube ayant un diamètre égal à celui du trou dans la maille. Des visualisations d'écoulement confirment l'existence de la maille hexagonale.

WÄRMEÜBERGANGSKOEFFIZIENTEN AN DER ANSTRÖMSEITE EINER GELOCHTEN UND SENKRECHT ZUR STRÖMUNG AUSGERICHTETEN PLATTE

Zusammenfassung—Es werden Experimente zur Bestimmung von Wärmeübergangskoeffizienten an einer gegen die Strömung gerichteten Platte durchgeführt, in die Löcher in regelmäßiger Anordnung gebohrt sind. Die Löcher sind in Form gleichseitiger Dreiecke angeordnet. Diese regelmäßige Geometrie läßt ein symmetrisches Strömungsbild vermuten, wobei jedes Loch von einem hexagonalen Gebiet umgeben ist, dessen Grenzen Symmetrielinien sind. Innerhalb eines jeden solchen hexagonalen Moduls sind die Wärmeübergangs- und Strömungsvorgänge gleich denen der anderen Module, welche die Fläche überdecken, so daß Messungen an einem einzelnen Modul die Information für die gesamte Fläche ergeben. Diese Eigenschaft wurde bei der Planung und Durchführung der beschriebenen Experimente ausgenutzt. Es wurden zwei Parameter bei den Messungen variiert—das Verhältnis Lochteilung zu Lochdurchmesser P/D und die auf das einzelne Loch bezogene Reynolds-Zahl Re. Die Ergebnisse werden von der Beziehung $Nu_L^* = 0{,}881\ Re^{0.476}\ Pr^{1/3}$ wiedergegeben. Die charakteristische geometrische Größe in der Nusselt-Zahl ist das Verhältnis der Moduloberfläche zur Teilung. Die Reynolds-Zahl entspricht der einer Rohrströmung mit dem Durchmesser der Löcher in der Platte als charakteristischer Länge. Die Sichtbarmachung der Strömung bestätigte die Existenz von hexagonal angeordneten Moduln.

КОЭФФИЦИЕНТЫ ТЕПЛОПЕРЕНОСА ОБРАЩЕННОЙ К ПОТОКУ ПОВЕРХНОСТИ ПЕРФОРИРОВАННОЙ ПЛАСТИНЫ, РАСПОЛОЖЕННОЙ ПОД ПРЯМЫМ УГЛОМ НАТЕКАНИЯ

Аннотация — Проведено экспериментальное определение коэффициентов теплопереноса на обращенной к потоку поверхности с регулярно расположенными рядами отверстий. Отверстия располгались в центрах равносторонних треугольников, что позволяло получить такую симметрию, при которой вокруг каждого отверстия можно выделить гексагональную область, границы которой являются линиями симметрии. Теплообменные и гидродинамические характеристики каждого такого гексагонального модуля идентичны характеристикам остальных модулей на поверхности, так что измерения, проведенные для одного модуля, дают информацию о всей поверхности. Эта особенность использовалась при постановке и проведении описанных экспериментов. В экспериментах изменялись два параметра: отношение шага отверстий к диаметру, P/D, и число Рейнольдса для каждого отверстия. Результаты обобщались с помощью соотношения $Nu_{L^*} = 0{,}881 Re^{0.476} Pr^{1/3}$. За характерный размер для числа Нуссельта принималось отношение площади поверхности модуля к шагу, а для числа Рейнольдса — линейный размер, характерный для течения в трубе с диаметром, равным диаметру отверстий в пластине. Визуализация течения подтвердила наличие рядов гексагональных модулей.